An inconditionnally stable discontinuous Galerkin method for solving the 2D time-domain Maxwell equations on unstructured triangular meshes

Adrien Catella, Victorita Dolean, Stephane Lanteri

An unconditionally stable discontinuous Galerkin method for solving the 2D time-domain Maxwell equations on unstructured triangular meshes

Adrien Catella, Victorita Dolean and Stéphane Lanteri

***Abstract*—Numerical methods for solving the time-domain Maxwell equations often rely on cartesian meshes and are variants of the finite difference time-domain (FDTD) method due to Yee [1]. In the recent years, there has been an increasing interest in discontinuous Galerkin time-domain (DGTD) methods dealing with unstructured meshes since the latter are particularly well adapted to the discretization of geometrical details that characterize applications of practical relevance. However, similarly to Yee's finite difference time-domain method, existing DGTD methods generally rely on explicit time integration schemes and are therefore constrained by a stability condition that can be very restrictive on locally refined unstructured meshes. An implicit time integration scheme is a possible strategy to overcome this limitation. The present study aims at investigating such an implicit DGTD method for solving the 2D time-domain Maxwell equations on non-uniform triangular meshes.**

***Index Terms*—time-domain Maxwell's equations, discontinuous Galerkin method, implicit time integration, local refinement, unstructured mesh.**

I. Introduction

In the numerical treatment of the time-domain Maxwell equations, finite difference time-domain (FDTD) methods based on Yee's scheme [1] are still prominent because of their simplicity (a time explicit method defined on cartesian meshes) and their non-dissipative nature (they hold an energy conservation property which is an important ingredient in the numerical simulation of unsteady wave propagation problems). Unfortunately, when dealing with complex geometries, the FDTD method is not always the best choice since a local refinement of the grid, albeit possible through a subgridding technique [2], has an adverse effect on accuracy and efficiency. In particular, local refinement can translate in a very restrictive time step in order to preserve the stability of the explicit leap-frog scheme used for time integration in the FDTD method. Finite element time-domain (FETD) methods based on unstructured meshes can easily deal with complex geometries however they induce heavy computations or require accurate and efficient lumping of mass matrices [3]. Finite volume time-domain (FVTD) methods on unstructured meshes also appeared as an alternative to FDTD methods, but they suffer from numerical diffusion resulting from the use of upwind schemes [4], and their extension to high-order accuracy is a tedious task. Discontinuous Galerkin time-domain (DGTD) methods can handle unstructured meshes and deal with discontinuous coefficients and solutions [5]. They can be seen as generalizations of the FVTD methods, where the finite element approximation is piecewise constant inside elements. The different achievements of the FVTD methods are now being extended in the context of DGTD methods which enjoy a renewed favor nowadays and are used in a wide variety of applications [6] as people rediscover the abilities of these methods to handle complicated geometries, media and meshes, to achieve a high order of accuracy by simply choosing suitable basis functions, to allow long-range time integrations and, last but not least, to remain highly parallelizable. However, DGTD methods suffer from the same limitation concerning the allowable time step on locally refined unstructured meshes. In this study, we investigate the applicability of an implicit time integration strategy in order to overcome the stability constraint which characterize explicit DGTD methods in the context of the numerical resolution of two-dimensional Maxwell's equations on locally refined unstructured triangular meshes.

A. Catella and S. Lanteri are with INRIA, 06902 Sophia Antipolis, France (e-mail: {Adrien.Catella, Stephane.Lanteri}@inria.fr).

V. Dolean is with the Nice/Sophia Antipolis University, J.A. Dieudonné Mathematics Lab., UMR CNRS 6621, 06108 Nice, France (e-mail: Victorita.Dolean@unice.fr).

The authors gratefully acknowledge support from CEA/CESTA under grant No. 4600 118950.

Manuscript received June 24, 2007.

II. Implicit DGTD method

The starting point of this study is the explicit DGTD method presented in [5] for solving the time-domain Maxwell equations on simplicial meshes. Beside a standard discontinuous Galerkin formulation, this method is based on two basic ingredients: a centered approximation for the calculation of numerical fluxes at inter-element boundaries, and an explicit leap-frog time integration scheme. The implicit DGTD method proposed here differs from its explicit counterpart in the time integration scheme which is now chosen to be a Crank-Nicolson scheme. We consider the two-dimensional Maxwell equations in the TMz polarization on a bounded domain $\Omega \subset \mathbb{R}^2$:

$$\begin{cases} \epsilon \dfrac{\partial E_z}{\partial t} - \dfrac{\partial H_y}{\partial x} + \dfrac{\partial H_x}{\partial y} = 0, \\ \mu \dfrac{\partial H_x}{\partial t} + \dfrac{\partial E_z}{\partial y} = 0, \quad \text{and} \quad \mu \dfrac{\partial H_y}{\partial t} - \dfrac{\partial E_z}{\partial x} = 0, \end{cases} \tag{1}$$

with boundary conditions $n\times E=0$ on Γ_m and $n\times E - zn\times(H\times n) = n\times E^{\text{inc}} - zn\times(H^{\text{inc}}\times n)$ on Γ_a where $\Gamma_a \bigcup \Gamma_m = \partial\Omega$, being $z=\sqrt{\mu/\varepsilon}$ the impedance. We assume a partition $\mathcal{T}_h$ of Ω into a set of triangles T_i and we seek for approximate solutions to (1) in the finite dimensional space $V_p(\mathcal{T}_h) := \{v \in L^2(\Omega) : v_{|T_i} \in \mathbb{P}_p(T_i)\ ,\ \forall T_i \in \mathcal{T}_h\}$, where $\mathbb{P}_p(T_i)$ denotes the space of nodal polynomials $\{\varphi_{ij}\}_{j=1}^d$ of total degree at most p on the element T_i. The space $V_p(\mathcal{T}_h)$ has the dimension d, the local number of degrees of freedom. Note that a function $v_h^p \in V_p(\mathcal{T}_h)$ is discontinuous across element interfaces. For two distinct triangles T_i and T_k in $\mathcal{T}_h$, the intersection $T_i \cap T_k$ is an (oriented) edge a_{ik} which we will call interface, with oriented normal vector $\vec{n}_{ik}$. For the boundary interfaces, the index k corresponds to a fictitious element outside the domain. Finally, we denote by $\mathcal{V}_i$ the set of indices of the elements neighboring T_i. The DGTD-$\mathbb{P}_p$ method at the heart of this study is based on a Crank-Nicolson time scheme and totally centered numerical fluxes at the interface between elements. Decomposing H_x, H_y and E_z on element T_i according to:

$$H_{\mathbf{x}}(.,t^n) = \sum_{j=1}^{d} H^n_{\mathbf{x}_{ij}}\varphi_{ij}, \quad E_z(.,t^n) = \sum_{j=1}^{d} E^n_{z_{ij}}\varphi_{ij},$$

where $\mathbf{x} \in \{x,y\}$. Using the notations $\mathbf{E}^n_{z_i} = (E^n_{z_{i1}},\ldots,E^n_{z_{id}})^t$ and $\mathbf{H}^n_{\mathbf{x}_i} = (H^n_{\mathbf{x}_{i1}},\ldots,H^n_{\mathbf{x}_{id}})^t$, the implicit DGTD-$\mathbb{P}_p$ method writes:

$$\begin{cases} \epsilon_i\mathbb{M}_i\dfrac{\mathbf{E}^{n+1}_{z_i}-\mathbf{E}^n_{z_i}}{\Delta t} & = -\mathbb{K}^x_i\mathbf{H}^{n+\frac12}_{y_i} + \mathbb{K}^y_i\mathbf{H}^{n+\frac12}_{x_i} \\ & \quad + \displaystyle\sum_{k\in\mathcal{V}_i}\left(\mathbb{G}^{n+\frac12}_{x_{ik}} - \mathbb{G}^{n+\frac12}_{y_{ik}}\right), \\ \mu_i\mathbb{M}_i\dfrac{\mathbf{H}^{n+1}_{x_i}-\mathbf{H}^n_{x_i}}{\Delta t} & = \mathbb{K}^y_i\mathbf{E}^{n+\frac12}_{z_i} - \displaystyle\sum_{k\in\mathcal{V}_i}\mathbb{F}^{n+\frac12}_{y_{ik}}, \\ \mu_i\mathbb{M}_i\dfrac{\mathbf{H}^{n+1}_{y_i}-\mathbf{H}^n_{y_i}}{\Delta t} & = -\mathbb{K}^x_i\mathbf{E}^{n+\frac12}_{z_i} + \displaystyle\sum_{k\in\mathcal{V}_i}\mathbb{F}^{n+\frac12}_{x_{ik}}, \end{cases}$$

being $\mathbb{M}_i$ the local mass (symmetric positive definite) matrix, and $\mathbb{K}^{\mathbf{x}}_i$ the (skew-symmetric) stiffness matrix. The vector quantities $\mathbb{F}^{n+\frac12}_{\mathbf{x}_{ik}}$ and $\mathbb{G}^{n+\frac12}_{\mathbf{x}_{ik}}$ are defined as:

$$\mathbb{F}^{n+\frac12}_{\mathbf{x}_{ik}} = \mathbb{S}^{\mathbf{x}}_{ik}\mathbf{E}^{n+\frac12}_{z_k}, \quad \mathbb{G}^{n+\frac12}_{\mathbf{x}_{ik}} = \mathbb{S}^{\mathbf{x}}_{ik}\mathbf{H}^{n+\frac12}_{\mathbf{x}_k},$$

where $\mathbb{S}^{\mathbf{x}}_{ik}$ is the $d\times d$ interface matrix on a_{ik} which verifies ${}^t\mathbb{S}^{\mathbf{x}}_{ik} = -\mathbb{S}^{\mathbf{x}}_{ki}$ (if a_{ik} is an internal interface) and ${}^t\mathbb{S}^{\mathbf{x}}_{ik} = \mathbb{S}^{\mathbf{x}}_{ik}$ (if a_{ik} is a boundary interface). Moreover:

$$\mathbf{E}^{n+\frac12}_{z_k} = \frac{\mathbf{E}^n_{z_k}+\mathbf{E}^{n+1}_{z_k}}{2} \quad \text{and} \quad \mathbf{H}^{n+\frac12}_{\mathbf{x}_k} = \frac{\mathbf{H}^n_{\mathbf{x}_k}+\mathbf{H}^{n+1}_{\mathbf{x}_k}}{2}.$$

In [7], we prove that the resulting implicit DGTD-$\mathbb{P}_p$ method is non-dissipative (if $\Gamma_a = \emptyset$) and unconditionally stable. This method requires the resolution of a sparse linear system at each time step but, for non-dispersive materials, the coefficient of this system are time independent, a feature that can be taken into account to minimize the additional computational overheadand. Thus, we have adopted here a multifrontal sparse matrix direct solver [8]. The sparse matrix characterizing the implicit DGTD-$\mathbb{P}_p$ method has a block structure where the size of a block is $3n_p \times 3n_p$, n_p being the number of degrees of freedom associated to a nodal polynomial basis of the space $\mathbb{P}_p$ i.e $n_p = ((p+1)(p+2))/2$. This matrix is factored once for all before the time stepping loop. Then, each linear system inversion amounts to a forward and a backward solve using the triangular L and U factors.

III. Numerical results

The numerical results presented here aim at comparing the explicit leap-frog based DGTD-$\mathbb{P}_p$ method and the implicit Crank-Nicolson based DGTD-$\mathbb{P}_p$ method. Simulations are performed on a personal workstation equipped with an AMD Opteron 2 GHz processor.

A. Eigenmode in a metallic cavity

The first test case that we consider is the propagation of an eigenmode in a unitary square cavity with perfectly conducting (PEC) walls. This test case allows a direct comparison with an exact solution. Here, it will also be used to demonstrate both the limitations in terms of accurarcy of the implicit DGTD-$\mathbb{P}_p$ method if the underlying mesh is uniform (or quasi-uniform) and the potential gains in CPU times that one can expect in the case of a non-uniform mesh. For this purpose, we make use of two triangular meshes:

- a uniform mesh consisting of 1681 vertices and 3200 triangles. The non-dimensioned time step corresponding to CFL-$\mathbb{P}_0$=1 is $(\Delta t)_u = 0.017678$ m (the physical time step is defined by $(\Delta t)_u = (\Delta t)_u/3.10^8$ m/s). For the interpolation orders $p \geq 1$, the time step actually used is CFL-$\mathbb{P}_p \times (\Delta t)_u$ where CFL-$\mathbb{P}_p$ is the CFL number associated to the DGTD-$\mathbb{P}_p$ method.
- a non-uniform mesh consisting of 1400 vertices and 2742 triangles. The ratio between the largest and smallest edges of this mesh is 178. In this case, the minimum and maximum values of the time step are respectively given by $(\Delta t)_m = 0.000434$ m and $(\Delta t)_M = 0.070617$ m. The time step used in the simulations is CFL-$\mathbb{P}_p \times (\Delta t)_m$.

For the explicit DGTD-$\mathbb{P}_p$ method, CFL-$\mathbb{P}_p \leq 1$ and the actual value is dictated by stability issues while CFL-$\mathbb{P}_p$ can be set to an arbitrarily large value for the implicit DGTD-$\mathbb{P}_p$ method but is constrained in practice by accuracy issues. Here, we only report on results obtained using the explicite and implicit DGTD-$\mathbb{P}_1$ methods. On Fig. 1 we have represented the time evolutions of the L2 error between the numerical and exact solutions. CPU times are given in Tab. I. Two main remarks can be made:

- although the implicit DGTD-$\mathbb{P}_p$ method is unconditionally stable, the CFL (and thus the time step) must be selected in order to ensure that the resulting solution is not altered by an increased level of dispersion error.
- as expected, the overhead introduced by the resolution of a linear system at each time step is minimized for large values of the CFL. Then the goal is to find a good compromise between the accuracy of the calculation and the required computational effort.

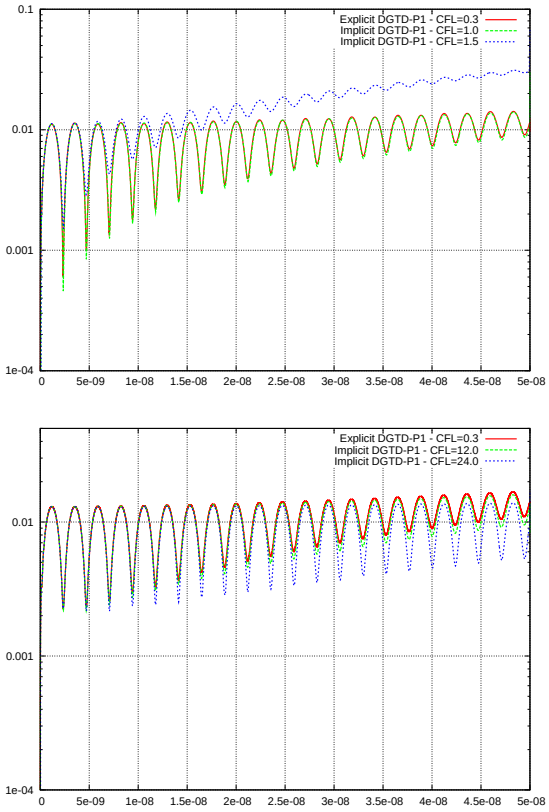

Fig. 1. Eigenmode in a PEC cavity. Time evolution of the L^2 error. Comparison between explicit and implicit DGTD-$\mathbb{P}_1$ methods. Uniform mesh (top) and non-uniform mesh (bottom).

TABLE I
EIGENMODE IN A PEC CAVITY: CPU TIMES.

Uniform triangular mesh

Time integration	Method	CFL-$\mathbb{P}_p$	CPU time
Explicit	DGTD-$\mathbb{P}_1$	0.3	15 sec
Implicit	-	1.0	44 sec
-	-	1.5	30 sec

Non-uniform triangular mesh

Time integration	Method	CFL-$\mathbb{P}_p$	CPU time
Explicit	DGTD-$\mathbb{P}_1$	0.3	443 sec
Implicit	-	12.0	133 sec
-	-	24.0	67 sec

B. Scattering of a plane wave by a square

The second test case that we consider is the scattering of a plane wave by a perfectly conducting square of side length c $= 0.25$ m. The farfield boundary Γ_a where the first order Silver-Müler absorbing condition is applied is defined as a square of side length c $= 1.0$ m. We make use of a non-uniform mesh consisting of 6018 vertices and 10792 triangles (see Fig. 2). The ratio between the largest and smallest edges is 357. In this case, the minimum and maximum values of the time step are respectively given by $(\Delta t)_m = 0.000286$ m and $(\Delta t)_M = 0.098589$ m. As previously, the time step used in the simulations is CFL-$\mathbb{P}_p \times (\Delta t)_m$. Simulations have been conducted for three frequencies of the incident plane wave, F=300 MHz, F=600 MHz and F=900 MHz and have been carried out for then periods. A discrete Fourier transform is applied to the field components during the last period.

Results are shown on Fig. 3 and 4 in terms of the x-wise 1D distribution for $y = 0.25$ m of the discrete Fourier transform (DFT) of E_z and for two frequencies (F=600 MHz and F=900 MHz). For each configuration, we show the distribution of DFT(E_z) for the time explicit calculation which is considered here as the reference solution, and two distributions of DFT(E_z) corresponding to time implicit calculations using respectively the maximum allowable CFL yielding a solution that fit the reference one, and a larger CFL yielding a less accurate solution. Computing times are summarized in Tab. II. These results call for two main remarks:

- as expected, the maximum allowable CFL value decreases when the frequency of the incident plane wave increases. Not surprisingly, despite the fact that the implicit DGTD-$\mathbb{P}_p$ method is unconditionally stable, the maximum allowable CFL value is deduced from physical considerations.
- as a result, for a given interpolation order, the gain in CPU time i.e the ratio of CPU time of the explicit DGTD-$\mathbb{P}_p$ calculation to the CPU time of the implicit DGTD-$\mathbb{P}_p$ calculation, decreases when the frequency increases. For instance, for $p = 2$ this ratio ranges from 7.5 for F=300 MHz to 3.0 for F=900 MHz. However, for a given frequency, this gain increases with the interpolation order: for F=900 MHz, this ratio is respectively equal to 3.0 for $p = 2$ and 5.5 for $p = 3$.

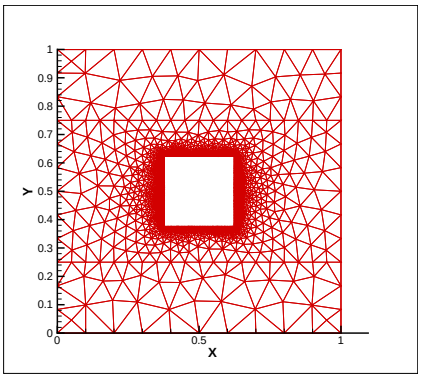

Fig. 2. Scattering of a plane wave by a PEC square: triangular mesh

TABLE II
SCATTERING OF A PLANE WAVE BY A PEC SQUARE: CPU TIMES.

Frequency	Time integration	Method	CFL-$\mathbb{P}_p$	CPU time
300 MHz	Explicit	DGTD-$\mathbb{P}_1$	0.3	1602 sec
-	Implicit	-	15.0	370 sec
-	Explicit	DGTD-$\mathbb{P}_2$	0.2	5677 sec
-	Implicit	-	15.0	762 sec
600 MHz	Explicit	DGTD-$\mathbb{P}_1$	0.3	758 sec
-	Implicit	-	7.0	383 sec
-	Explicit	DGTD-$\mathbb{P}_2$	0.2	3074 sec
-	Implicit	-	7.0	767 sec
900 MHz	Explicit	DGTD-$\mathbb{P}_2$	0.2	2191 sec
-	Implicit	-	5.0	746 sec
-	Explicit	DGTD-$\mathbb{P}_3$	0.1	8771 sec
-	Implicit	-	5.0	1591 sec

IV. Conclusion and future works

We have studied here an implicit DGTD-$\mathbb{P}_p$ method for solving the time-domain Maxwell equations on triangular meshes. The method is non-dissipative, second order accurate in time an p-th order accurate in space. As usual with time implicit schemes, this method requires the resolution of a sparse linear system at each time step. In the present case, the coefficients of the matrix are constant in time. Taking into account this feature in the linear system solution strategy is a key ingredient for obtaining a computationally efficient method. For two-dimensional problems, a direct solver based on a LU factorization such as the one adopted in this study is generally considered as the optimal strategy, at least from the computing time point of view. Promising results have been obtained for time-domain electromagnetic wave propagation problems on locally refined unstructured meshes. Concerning future works, our main objective will be to adapt the implicit DGTD-$\mathbb{P}_p$ method proposed here to the case of the three-dimensional time-domain Maxwell equations. In this context, it is clear that a global direct solver such as the multifrontal method adopted in this study will not be an acceptable option due to the large memory capacity required for the simulation of realistic three-dimensional problems, especially if the computational domain is discretized using unstructured tetrahedral meshes. In this context, parallel computing will be a mandatory path and although MUMPS [8] is a parallel sparse matrix solver, we plan to consider a Schwarz type domain decomposition method [9] as a mean to build an hybrid iterative/direct solver, and still benefit from the fact that the sparse matrix associated to a sub-domain problem can be factored once for all before the time stepping loop.

References

[1] K. Yee, "Numerical solution of initial boundary value problems involving Maxwell's equations in isotropic media," *IEEE Trans. Antennas and Propagat.*, vol. 14, no. 3, pp. 302–307, 1966.

[2] S. Chaillou, J. Wiart, and W. Tabbara, "A subgridding scheme based on mesh nesting for the FDTD method," *Microwave and Optical Technology Letters*, vol. 22, no. 3, pp. 211–214, 1999.

[3] S. Pernet, X. Ferrieres, and G. Cohen, "High spatial order finite element method to solve Maxwell's equations in time domain," *IEEE Trans. on Antennas and Propagation*, vol. 53, no. 9, pp. 2889–2899, 2005.

[4] J.-P. Cioni, L. Fezoui, L. Anne, and F. Poupaud, "A parallel FVTD Maxwell solver using 3D unstructured meshes," in *13th Annual Review of Progress in Applied Computational Electromagnetics*, Monterey, CA, USA, 1997, pp. 359–365.

[5] L. Fezoui, S. Lanteri, S. Lohrengel, and S. Piperno, "Convergence and stability of a discontinuous Galerkin time-domain method for the heterogeneous Maxwell equations on unstructured meshes," *ESAIM: Math. Model. and Numer. Anal.*, vol. 39, no. 6, pp. 1149–1176, 2006.

[6] B. Cockburn, G. Karniadakis, and C. Shu, Eds., *Discontinuous Galerkin methods. Theory, computation and applications*, ser. Lecture Notes in Computational Science and Engineering. Springer-Verlag, 2000, vol. 11.

[7] A. Catella, V. Dolean, and S. Lanteri, "An implicit DGTD method for solving the two-dimensional Maxwell equations on unstructured triangular meshes," INRIA, Tech. Rep. RR-6110, 2006. [Online]. Available: https://hal.inria.fr/inria-00126573

[8] P. Amestoy, I. Duff, and J.-Y. L'Excellent, "Multifrontal parallel distributed symmetric and unsymmetric solvers," *Comput. Meth. App. Mech. Engng.*, vol. 184, pp. 501–520, 2000.

[9] V. Dolean, L. Gerardo-Giorda, and M. Gander, "Optimized Schwarz methods for Maxwell equations," 2006. [Online]. Available: https://hal.archives-ouvertes.fr/ccsd-00107263

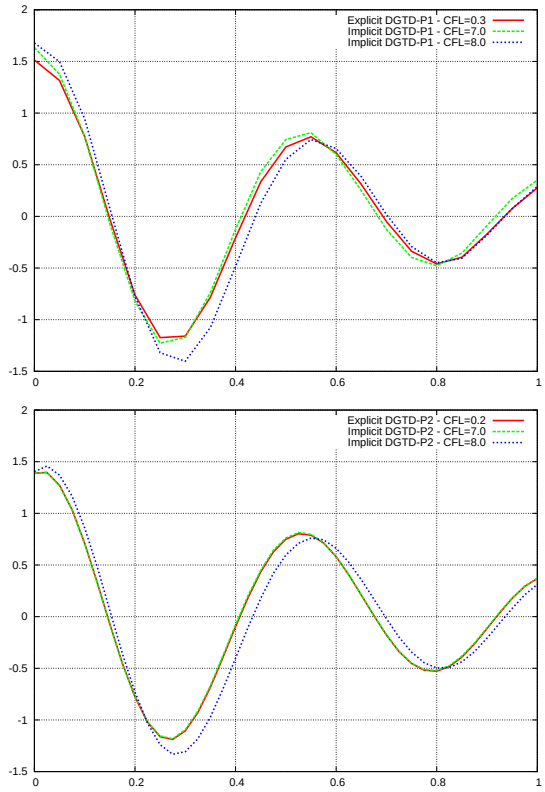

Fig. 3. Scattering of a plane wave by a PEC square, F=600 MHz. 1D distribution of DFT(E_z), $y = 0.75$ m. DGTD-$\mathbb{P}_1$ method (top) and DGTD-$\mathbb{P}_2$ method (bottom).

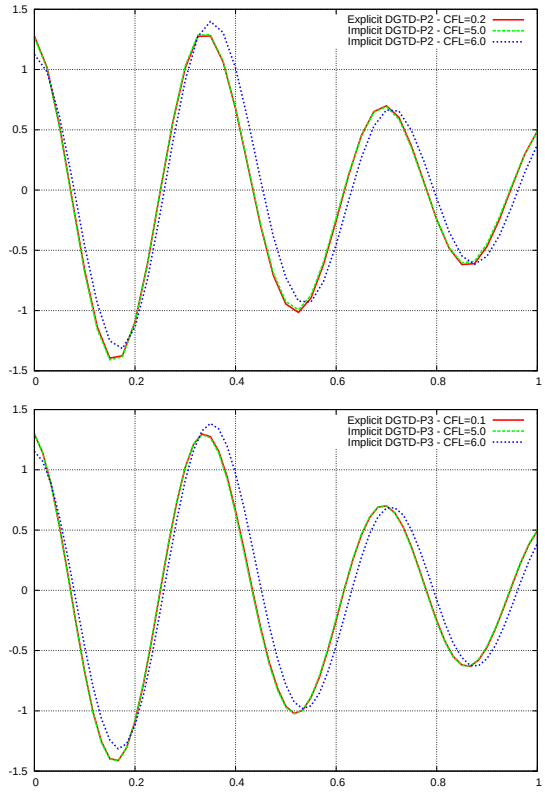

Fig. 4. Scattering of a plane wave by a PEC square, F=900 MHz. 1D distribution of DFT(E_z), $y = 0.75$ m. DGTD-$\mathbb{P}_2$ method (top) and DGTD-$\mathbb{P}_3$ method (bottom).